Sawtooth control in fusion plasmas

J P Graves[1], **C Angioni**[2], **R V Budny**[3], **R J Buttery**[4], **S Coda**[1],
L-G Eriksson[5], **C G Gimblett**[4], **T P Goodman**[1], **R J Hastie**[4],
M A Henderson[1], **H R Koslowski**[6], **M J Mantsinen**[7], **An Martynov**[1],
M-L Mayoral[4], **A Mück**[1], **M F F Nave**[8], **O Sauter**[1], **E Westerhof**[9] **and**
JET–EFDA Contributors[10]

[1] Centre de Recherches en Physique des Plasmas, Association EURATOM—Confédération
Suisse, EPFL, 1015 Lausanne, Switzerland
[2] MPI für Plasmaphysik, EURATOM—Association, D-85748 Garching, Germany
[3] Princeton Plasma Physics Laboratory, Princeton, NJ 08543, USA
[4] Euratom/UKAEA Fusion Association, Culham Science Centre, Abingdon,
Oxon OX14 3DB, UK
[5] Association EURATOM-CEA, CEA/DSM/DRFC, CEA-Cadarache, F-13108 St. Paul lez
Durance, France
[6] Association EURATOM-FZ-Juelich, Institut fuer Plasmaphysik, Trilateral Euregio Cluster,
D-52425 Juelich, Germany
[7] Association Euratom—Tekes, Helsinki University of Technology, Finland
[8] Associação EURATOM/IST, Centro de Fusão Nuclear, Lisbon, Portugal
[9] FOM—Institute for Plasma Physics Rijnhuizen, Association EURATOM-FOM, Trilateral
Euregio Cluster, The Netherlands

Abstract
Clear observations of early triggering of neo-classical tearing modes by
sawteeth with long quiescent periods have motivated recent efforts to control,
and in particular destabilize, sawteeth. One successful approach explored
in TCV utilizes electron cyclotron heating in order to locally increase the
current penetration time in the core. The latter is also achieved in various
machines by depositing electron cyclotron current drive or ion cyclotron current
drive close to the $q = 1$ rational surface. Crucially, localized current drive
also succeeds in destabilizing sawteeth which are otherwise stabilized by a
co-existing population of energetic trapped ions in the core. In addition, a
recent reversed toroidal field campaign at JET demonstrates that counter-neutral
beam injection (NBI) results in shorter sawtooth periods than in the Ohmic
regime. The clear dependence of the sawtooth period on the NBI heating
power and the direction of injection also manifests itself in terms of the toroidal
plasma rotation, which consequently requires consideration in the theoretical
interpretation of the experiments. Another feature of NBI, expected to be
especially evident in the negative ion based neutral beam injection (NNBI)
heating planned for ITER, is the parallel velocity asymmetry of the fast ion

[10] See appendix in Pamela J *et al* 2004 *Proc. 20th IAEA Conf. on Fusion Energy 2004 (Vilamoura, Portugal, 2004)*.

population. It is predicted that a finite orbit effect of asymmetrically distributed circulating ions could strongly modify sawtooth stability. Furthermore, NNBI driven current with non-monotonic profile could significantly slow down the evolution of the safety factor in the core, thereby delaying sawteeth.

(Some figures in this article are in colour only in the electronic version)

1. Introduction

The control of sawteeth is expected to be important in a next step device such as ITER [1]. The presence of highly energetic ions in large tokamaks has given rise to sawteeth with long quiescent times and large amplitudes [2–4]. Although this might seem to be an advance, large sawteeth also have detrimental ramifications. In particular, the radial location of the collapse event propagates with respect to the sawtooth quiescent time. The collapse radius has been predicted to be so large in ITER [5] that coupling is likely to occur with modes at other rational surfaces. Evidence of interaction between large sawteeth and 3/2 neoclassical tearing modes (NTMs) has been observed in JET [6], while discharges with smaller regular sawteeth are found to have increased core confinement and are less likely to be coupled to confinement degrading NTMs [6]. Hence it is seen that greater understanding and control over the mechanisms that determine sawteeth stability are required.

Sawtooth control refers to the ability of an actuator system, i.e. some additional heating and/or current drive, to alter the period and usually the amplitude of the sawtooth instability. Two strategies are possible to avoid the deleterious effects of large sawteeth. One option which has had some success in JET [7] is the attempt to suppress sawteeth for many energy confinement times. In ITER one would attempt to reach burning conditions before the onset of the first crash. This may prove possible because of the expected stabilizing properties of the trapped alpha population [8]. Moreover, as we shall discuss later, co-injection of negative ion based neutral beams in ITER's baseline scenario could suppress the formation of a $q = 1$ rational surface over a significant fraction of the current penetration timescale. The other strategy is to deliberately increase the rate of sawteeth, i.e. destabilize sawteeth, in order to reduce the perturbation to the plasma beyond the inversion radius. The most successful and repeatable experiments involve radio frequency (RF) heating and current drive with the resonant surface localized close to the $q = 1$ rational surface. Evidently the control mechanism involves the destabilizing effect of creating local perturbations in the current and electron temperature profiles [9, 10]. Another approach involves the injection of neutral beams with orientation opposite to the direction of the plasma current [11]. Such experiments point to the possible sensitivity of sawteeth to momentum induced plasma rotation.

This paper collects recent experiments and simulations which employ localized electron cyclotron heating (ECH) and current drive (ECCD) [10, 12, 13] and ion cyclotron resonance heating (ICRH) and current drive (ICCD) [6, 12, 14] to control sawteeth. The reproducibility of such experiments has recently been exploited in order to destabilize sawteeth by localized ICCD and thereby control sawteeth which were initially lengthened by a population of energetic ions in the core [15]. This has important and encouraging implications for the control of sawteeth in a next step tokamak, since the experiments provide evidence that local modification of the current profile could assist destabilization of sawteeth despite the predicted large energy sink δW from the kinetic contribution of trapped alpha particles in the core. Also presented in this paper are dedicated experiments and analysis of counter-injection (counter in relation to

the plasma current and toroidal field) of neutral beams in JET [16]. It will be seen that the observation of sawteeth in discharges employing moderate counter-NBI, with quiescent times not exceeding those of Ohmic discharges, can be partially explained in terms of a reduction in stabilizing kinetic contributions to δW. Finally, recent experimental [17] and theoretical [18] results on negative ion based neutral beam injection (NNBI) are reviewed. Despite NNBI populations having a dominant passing fraction, the sawteeth are strongly stabilized by the energetic population. It is shown in this paper under what conditions the NNBI ions could be as influential as alpha particles for sawtooth stabilization in ITER.

This paper is organized as follows: models for the sawtooth trigger and plasma evolution are overviewed in section 2; section 3 presents recent important progress on sawtooth control using localized current drive; in section 4 the effect of counter-NBI on sawteeth in JET is presented; section 5 gives a brief overview of our understanding of sawtooth control using NNBI and the last section contains concluding remarks on the work presented here.

2. Modelling the sawtooth instability

2.1. The trigger problem

The sawtooth trigger problem is addressed by seeking to correlate equilibrium properties at the onset of the $m = n = 1$ instability with the crossing of a theoretical stability boundary for the internal kink mode. The theoretical boundary differs as additional physical effects are added into the linearized 'MHD' equations.

It is found that the stability of sawteeth in TCV falls into two broad classes [19] depending on the shape of the plasma cross section. In particular, sawteeth were found to be small for plasmas with large elongation and/or small triangularity. We shall see that such plasma shaping strongly destabilizes MHD modes in the core plasma; this includes the internal kink mode, the ideal interchange mode and the resistive interchange mode. Since additional heating shortens the sawtooth period even further, it follows [19] that the sawtooth period for such equilibria could be triggered by the criterion for ideal instability:

$$\pi \frac{\widehat{\delta W}}{s_1} < -\frac{\omega_{*i}\tau_A}{2}$$

with ω_{*i} the ion diamagnetic frequency, s_1 the magnetic shear $s = (r/q)\partial q/\partial r$ evaluated at $q = 1$ (denoted by subscript '1'), $\widehat{\delta W} = \delta W/(2\pi^2\xi_0^2\epsilon_1^4 R_0 B_0^2/\mu_0)$ where δW and ξ_0 are, respectively, the perturbed potential energy and leading order displacement of the $m = n = 1$ mode and ϵ_1 is the inverse aspect ratio at $q = 1$. Here the ideal MHD growth rate $\gamma_1\tau_A = -\pi\widehat{\delta W}/s_1$, where $\widehat{\delta W}$ can in general account for MHD contributions $\widehat{\delta W}_{\text{MHD}}$ and kinetic contributions $\widehat{\delta W}_k$ from auxiliary hot ion populations and thermal ions in the banana regime. Increased heating would make the MHD contribution to $\widehat{\delta W}$ more unstable because toroidal contributions [20] and combined toroidal-shaping contributions [21] are increasingly destabilizing for increasing β_p, the poloidal beta at $q = 1$. The contributions to ideal MHD stability have recently been compiled in [22]:

$$\widehat{\delta W}_{\text{MHD}} = \Delta q \epsilon^2 3\left[\left(0.3 - 0.5\frac{\langle r\rangle}{\langle a\rangle}\right)^2 - \beta_p^2\right] + \epsilon^4\left[6\beta_p^3(1+\beta_p) + \frac{\beta_p(1-14\beta_p)}{32}\right] - \frac{3\Delta q^3}{2}e^2$$

$$+ \frac{\Delta q}{4}\delta^2 + e\epsilon^2\left\{-\frac{3}{2}\beta_p + \frac{\Delta q}{12}(156\beta_p^2 - 3\beta_p - 12)\right\} + e\delta\epsilon\left\{3\beta_p + \frac{\Delta q}{6}(4\beta_p - 7)\right\}$$
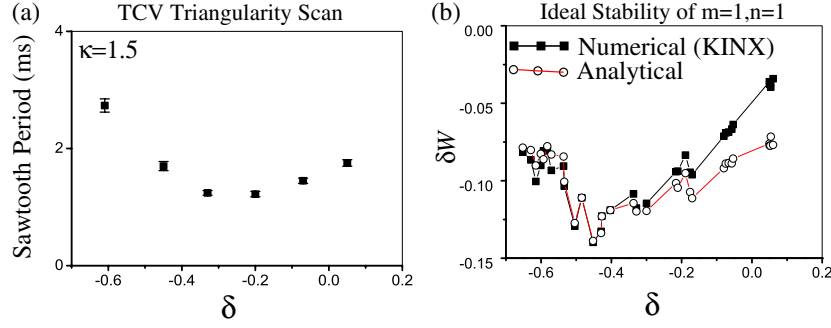
$$(1)$$

Figure 1. Plot of (*a*) the sawtooth period in TCV over large inward pointing to small conventional outward pointing triangularity for moderate elongation. The trend is very similar to (*b*) the ideal stability given by equation (1) and with results from the KINX ideal MHD stability code [22].

with $e = (\kappa - 1)(\kappa + 1)$, κ the elongation, δ the triangularity, $\langle r \rangle = r\kappa^{1/2}$, $\Delta q = 1 - q_0$ and all quantities are evaluated at r_1. Figure 1 plots the sawtooth period over a triangularity scan (ranging from large inward pointing to small outward pointing), together with a similar trend in $\widehat{\delta W}_{\text{MHD}}$ given above and the same quantity calculated numerically [22].

In contrast to the high κ, or small positive or negative δ scenarios mentioned above, for more conventional scenarios with moderate δ and κ, the sawtooth period in TCV increased with respect to increasing heating power [19]. Such a dependence on heating is consistent with the sawtooth trigger being described by resistive MHD with two fluid effects. Although the $m = n = 1$ instability is always unstable in one-fluid resistive MHD, accounting for two fluid effects in the layer reveals stable regions of parameter space which could account for quiescence during sawteeth [23]. The instability criterion can be written in the form $s_1 > s_{\text{c}}(\beta)$. In [5] it is pointed out that the effects in the layer, which are described by the latter critical shear criterion, are only important when the macroscopic drive $\widehat{\delta W}$ of the internal kink mode is not strongly stabilizing, i.e. there is not a very large energy sink. The criterion for instability is thus given by [5]

$$\pi \frac{\widehat{\delta W}}{s_1} < c_\rho \rho_{\text{i}} \tag{2}$$

and

$$s_1 > s_{\text{c}}(\beta), \tag{3}$$

where ρ_{i} is the ion Larmor radius normalized to the $q = 1$ radius, c_ρ a numerical constant of order unity and $s_{\text{c}}(\beta)$ is a critical shear, governed essentially by the pressure profile [5, 23–25]. The definition of $s_{\text{c}}(\beta)$ depends on the regime of interest. It is for example defined for instability in the ion kinetic regime, or resistive regime, by equations (5*b*) and (5*a*) of [12], respectively.

2.2. Plasma evolution during ramp phase

In order to interpret the sawtooth period in present day experiments, and predict the sawtooth period in planned regimes and future experiments, it is clear that the transport between sawteeth (the ramp phase) must be modelled accurately. An estimation of the current diffusion can be obtained upon considering the leading order tokamak expressions for the induction equation $\partial B_\theta / \partial t = E'_\phi$, Ohm's law $E_\phi \approx \eta j_{\text{Ohm}}$ and Amperes law $\mu_0(j_{\text{Ohm}} + j_{\text{cd}} + j_{\text{boot}}) = (rB_\theta)'$,

where $x' \equiv \partial x / \partial r$ and $j_{Ohm} + j_{cd} + j_{boot}$ is the total current, comprising the Ohmic current, driven current and bootstrap current. These equations can be written as an evolution equation in the poloidal magnetic field: $\partial B_\theta / \partial t = [(\eta/r)(rB_\theta/\mu_0)' - \eta(j_{cd} + j_{boot})]'$, where η is the resistivity, which scales with electron temperature as $\sim T_e^{-3/2}$. Now, for small shear, and using $q \approx rB_0/R_0 B_\theta$, one obtains

$$\frac{\partial q}{\partial t} = -\frac{q}{r}\left[\frac{2}{\mu_0}\frac{\partial \eta}{\partial r} - \frac{qR_0}{B_0}\frac{\partial}{\partial r}(\eta j_{cd} + \eta j_{boot})\right] \tag{4}$$

and assuming that $(\eta j)' \gg r(\eta j)''$:

$$\frac{\partial s}{\partial t} = \frac{2}{\mu_0 r}\frac{\partial \eta}{\partial r} - \frac{1}{B_\theta}\frac{\partial}{\partial r}(\eta j_{cd} + \eta j_{boot}). \tag{5}$$

Hence it is seen that variation of the deposition of current drive and/or the conductivity profile modifies the time it takes to reach the critical shear criterion of equation (3), and hence presumably the sawtooth period.

The effect of modifying the conductivity profile on sawteeth is demonstrated in figure 2. It is clear that the predictions of the effects of differing ECH sources are qualitatively and essentially quantitatively validated by these TCV discharges [12]. From equation (5) it is seen that heating outside the inversion radius, such that η' is reduced at r_1, reduces $\partial s / \partial t$ in turn (here inversion radius refers to the radius at which the temperature is unchanged over the crash event). Thus the data in figure 2 commence with long sawteeth. Another beam is deposited close to the magnetic axis and is then swept through the inversion radius. Again, from equation (5), the effect on the local conductivity profile initially gives rise to an increase in $\partial s / \partial t$, and as the beam crosses to the outside of the inversion radius, $\partial s / \partial t$ is strongly reduced. In the PRETOR-ST simulations [12], the variation in $\partial s / \partial t$ modifies the sawtooth period because of the differing timescales over which the critical shear criterion of equation (3) is reached. It should be noted that equation (2) is always satisfied for these experiments which are devoid of energetic minority ions.

It is recognized that simulations of the type shown in figure 2 assume Kadomsev [26] full reconnection at the crash. Consequently the transport during the ramping phase commences with $s = 0$ and $r_1 = 0$. Clearly, if full reconnection does not actually occur, transport during the ramp based on Kadomsev initial conditions would over-estimate the sawtooth period if other 'free' parameters (e.g. in $s_c(\beta)$) cannot be employed to artificially hasten the triggering event. A relaxation process which does not give rise to such a small shear at the end of the crash phase (and beginning of the next ramp) is based on Taylor relaxation [27]. The potential instability of high m, n resistive (e.g. tearing parity or twisting parity) modes within the region of resistive interchange instability is a justification for the Taylor relaxation model [27]. The growth of an $m = 1$ island could nevertheless be the primary instability which ultimately triggers the sawtooth. In particular, the $m = 1$ island could locally increase the pressure gradient drive of the resistive interchange mode when the growing separatrix of the $m = 1$ island intersects the region of resistive interchange instability. Sawtooth precursors would thus be observable until the island has grown sufficiently large. However, evaluation of the region of instability of the resistive interchange mode in MAST [28] indicates that the plasma is unstable beyond the $q = 1$ surface for elongated plasmas. For such a configuration, high m, n resistive modes could thus occur at a much earlier stage of the $m = 1$ island formation. A convincing demonstration of the relevance of resistive interchange instability, and ultimately Taylor relaxation, could be the observation of precursorless sawteeth in strongly elongated discharges and sawteeth with $m = 1$ precursors in more conventional (moderate triangularity and elongation) discharges.
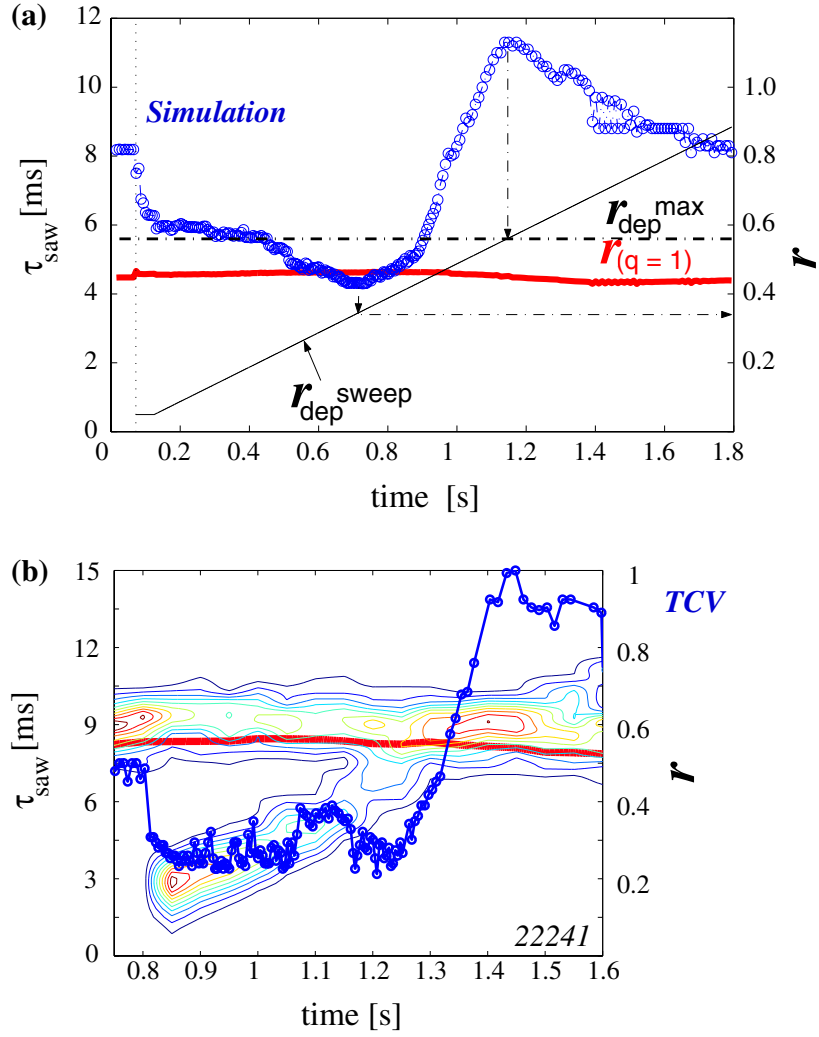
(a)

(b)

Figure 2. Showing (*a*) predictions of the sawtooth period using PRETOR-ST and (*b*) the measured sawtooth period in TCV with beams of ECH orientated just outside the $q = 1$ radius to stabilize the sawteeth, and another beam is then swept through the inversion radius [12]. Contours in (*b*) indicate location of heat deposited relative to minor radius r.

Pellet injection into the core quite frequently results in the creation of a high density closed tube of plasma on the $q = 1$ surface [29]. Observations [28] of these so-called snakes surviving consecutive crash events in the MAST experiments mentioned above indicate that the $q = 1$ radius undergoes only a small variation over the sawtooth cycle. It is important to note that evidence showing that full reconnection does not occur demands a high degree of temporal resolution. This follows because, immediately following Kadomsev reconnection, the rate of change of the $q = 1$ radius is initially very fast, due to its dependence on the vanishingly small magnetic shear:

$$\frac{dr_1}{dt} = \frac{1}{s} \left[\frac{2}{\mu_0} \frac{\partial \eta}{\partial r} - \frac{R_0}{B_0} \frac{\partial}{\partial r} (\eta j_{cd} + \eta j_{boot}) \right] \Bigg|_{r_1}.$$
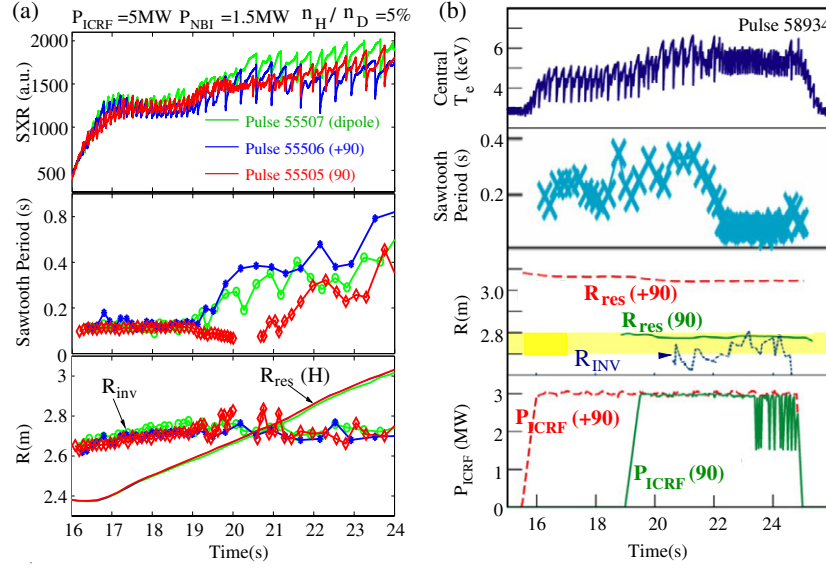
Figure 3. (*a*) Soft x-ray emission, sawtooth period, sawtooth inversion radius R_{inv} and first harmonic H cyclotron resonance layer $R_{res}(H)$ for three similar JET discharges [14] for which only the phasing of the ICRF wave was changed: $+90°$ phasing in pulse 55505, $-90°$ phasing in pulse 55506 and dipole phasing in 55507. (*b*) Pulse 58934 in JET [15], plotting the electron temperature, sawtooth period, sawtooth inversion radius R_{inv} and first harmonic H cyclotron resonance layer $R_{res}(H)$ for $+90°$ and $-90°$ phasings, and heating power for the two antennae.

3. Control of sawteeth by current drive

Experiments in TCV [10], and more recently in ASDEX-Upgrade [13], demonstrate that the addition of small amounts (less than a few per cent of the plasma current) of co-ECCD to ECH in the sweep in the resonance location enhances the trend observed in figure 2. This can be understood upon inspection of equation (5) where it is seen that co-current drive with resonance location outside $q = 1$, thus giving rise to $\partial j_{cd}\partial r|_{r_1} > 0$, slows down the evolution of s. Clearly, co-ECCD inside $q = 1$ reduces the sawtooth period. The variation of the plasma evolution and consequent sawtooth period is clearly demonstrated in simulations [12] which account for the combined effects of localized heating and current drive.

Perturbations in the current can also be obtained effectively with ICRH upon employing a particular choice of current phasing in the RF antennae [30]. Figure 3(*a*) shows recent results from JET [14] demonstrating the crucial differences between $-90°$, $+90°$ and dipole phasings over a magnetic field and plasma current scan in discharges employing first harmonic heating of minority hydrogen in a deuterium D(H) plasma on the high field side (HFS). A large region encompassing both sides of the inversion radius is distinguished within which the resonant surface can be localized in order to obtain large sawteeth for the case of $+90°$ and vanishingly small sawteeth for the $-90°$ case. Again these results are understood in terms of a change in the sign and magnitude of $\partial j_{cd}/\partial r$.

Unlike co-ECCD with resonant position inside $q = 1$, one does not see significant destabilization of sawteeth for the $+90°$ case as the resonant surface moves inside the inversion radius. As pointed out in [31] there are two competing mechanisms at work, namely the effect of the minority ions on the current perturbation and also the stabilizing effect of hot 'h' trapped

minority ions on the macroscopic potential energy:

$$\widehat{\delta W}_{\mathrm{kh}} = \frac{1}{\pi (2\epsilon_1)^{1/2}} \beta_{\mathrm{ph}} \qquad \text{with } \beta_{\mathrm{ph}} = -\frac{2\mu_0}{B_0^2} \int_0^{r_1} \mathrm{d}r \left(\frac{r}{r_1}\right)^{3/2} \frac{\mathrm{d}P_{\mathrm{h}}}{\mathrm{d}r}. \qquad (6)$$

This latter stabilizing effect is most significant for ions heated with the +90° phasing because these particles are pinched inwards towards the magnetic axis [32], thus creating larger fast ion pressure gradients within the $q = 1$ surface. Intuitively, the opposite occurs for the −90° phasing. Nevertheless, all three phasing conditions give rise to kinetic stabilization of the sawteeth as the resonant surface approaches the magnetic axis.

Crucial recent experiments in JET [15] demonstrate that creating current perturbations with $\partial j_{\mathrm{cd}}/\partial r < 0$ can control (destabilize) sawteeth even where the plasma additionally comprises a fast ion population in the core yielding a large stabilizing macroscopic drive of the form of equation (6). It is noted in [15] that despite this stabilizing contribution, increasing the magnetic shear can shorten the sawtooth period via the shear dependence in the macroscopic threshold for instability of the internal kink mode in the ion kinetic regime, i.e. equation (2). Shown in figure 3(b) are long sawteeth initially stabilized by using central hydrogen minority heating and +90° phasing. At 19 s the same species is also heated close to the inversion radius on the HFS with −90° phasing. As the discharge evolves, and the inversion radius converges with the hydrogen resonance position of the −90° phasing, the sawteeth become very short.

Clearly in ITER it may be necessary to use techniques to modify $s_1(t)$ in order to control sawteeth lengthened by the predicted large energy sink from the kinetic contribution of trapped alpha particles in the core. Indeed, evidence of seeding of NTMs through sawteeth lengthened by a He^4 population heated into the MeV range with third harmonic ICRH [33] confirms that this is likely to be crucial. The use of ITER relevant second harmonic ICCD [6] has been successful in controlling sawteeth and avoiding the triggering of NTMs with β_{N} close to the ideal MHD limit.

4. Counter NBI and toroidal rotation

In this section the influence of plasma rotation on sawteeth is considered. Figure 4 shows two otherwise similar recent JET discharges [16] which have opposite NBI orientation (relative to the direction of the toroidal plasma current and toroidal magnetic field). It is seen that the co-NBI discharge has increasingly large sawteeth for increasing heating power up to a maximum of $P_{\mathrm{NBI}} \approx 3.8\,\mathrm{MW}$, while the cntr-NBI discharge has sawteeth with quiescent periods close to the Ohmic timescale throughout the ramp up and ramp down in the neutral beam power.

A clear difference between the two discharges shown in figure 4 is the change in sign in the plasma rotation relative to the toroidal current and magnetic field. Figures 5(a) and (b) plot the measured differential toroidal plasma rotation $\Delta\Omega = -r\Omega'|_{r_1}$ and the ion diamagnetic frequency $\omega_{*\mathrm{pi}}(r_1)$ with respect to time for the shots shown in figure 5. Here $\Omega' = \mathrm{d}\Omega/\mathrm{d}r$ and $\omega_{*\mathrm{pi}} = -q P_{\mathrm{i}}'/(eZn_{\mathrm{i}}B_0 r)$. It is seen that for co-injection $\Delta\Omega \approx 2\omega_{*\mathrm{pi}}$, while for the counter-injection discharge $\Delta\Omega \approx -2\omega_{*\mathrm{pi}}$. This scaling of the differential plasma rotation relative to the ion diamagnetic frequency is required in order to assess the stabilizing contribution of effectively collisionless trapped ions. The response of the NBI hot 'h' ions to the internal kink mode is essentially given by equation (6) for such relatively small sheared flow [34] for which $\Delta\Omega \ll \{\langle\omega_{\mathrm{mdh}}\rangle, \omega_{*\mathrm{h}}\}$, where $\langle\omega_{\mathrm{mdh}}\rangle$ is the magnetic drift and $\omega_{*\mathrm{h}}$ the diamagnetic frequency of the hot ions. In contrast, the collisionless response of the thermal ions 'i' is significantly modified by sheared flow [35] because $\Delta\Omega \sim \{\langle\omega_{\mathrm{mdi}}\rangle, \omega_{*\mathrm{i}}\}$. Figure 5(c) plots the
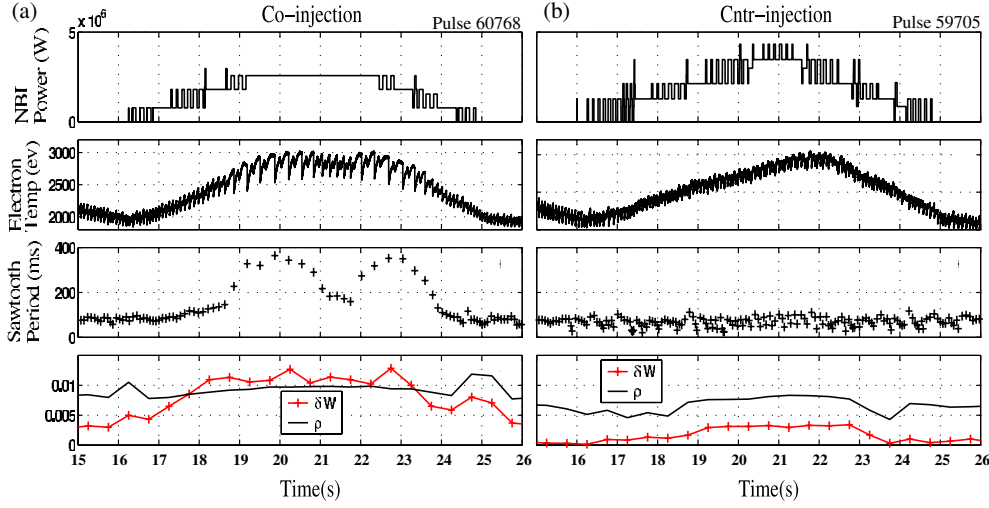
Figure 4. Showing two otherwise similar NBI ramping discharges with opposite NBI orientation [16]. Also compared are the expressions $\delta W = \pi \widehat{\delta W}/s_1$ and $\rho = c_\rho \rho_i$ in the macroscopic threshold instability criterion of equation (2).
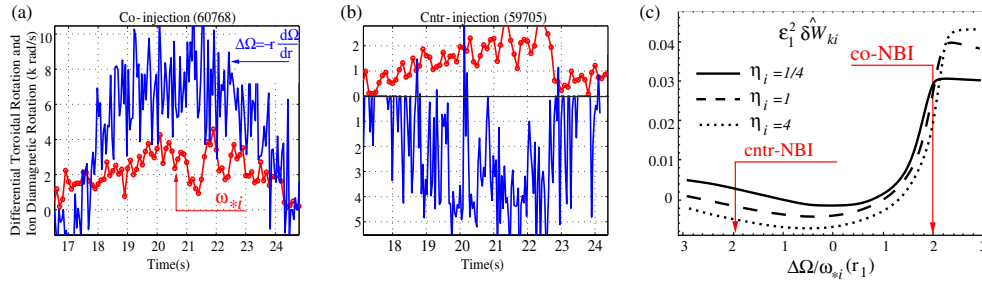

Figure 5. Showing $\Delta\Omega$ and ω_{*pi} for (a) the co-NBI and (b) the cntr-NBI discharges shown in figure 4. The variation of $\epsilon_1^2 \widehat{\delta W}_{ki}$ with respect to $\Delta\Omega/\omega_{*pi}$ is shown in (c).

kinetic contribution from thermal ions $\widehat{\delta W}_{ki}$ as a function of $\Delta\Omega/\omega_{*pi}$ for typical core plasma profiles and for differing $\eta_i = d\ln T_i/d\ln n_i$. Variation in $\Delta\Omega$ was undertaken by changing the central plasma rotation Ω_0 for a fixed profile $\Omega/\Omega_0 = 1 - (r/2a)^2$ as in [35]. Indicated in figure 5(c) are the approximate relevant normalized differential frequencies for the co- and cntr-NBI discharges depicted in figures 4(a) and (b). This serves to illustrate the influence of sheared flow on stability for the discharges of concern here.

Figure 4 also plots the terms involved in the criterion of equation (2) for the co-NBI discharge 60768 and reverse B discharge 59705. This is achieved by computing the time evolution of the quantities involved by taking data directly from the available JET diagnostics and post-processing codes such as PENCIL [36]. For the co-NBI case the large increase in the sawtooth period coincides with the approximate time during the ramp when the macroscopic instability criterion of equation (2) is no longer satisfied [24]. The sawtooth period essentially returns to an Ohmic timescale $\tau_{saw} \sim 80$ ms at the point during the ramp down phase when equation (2) is satisfied. Both δW_{ki} and δW_{kh} are responsible for the stabilization during the ramp. In contrast, for the cntr-NBI case, the sawtooth period does not rise above that of Ohmic
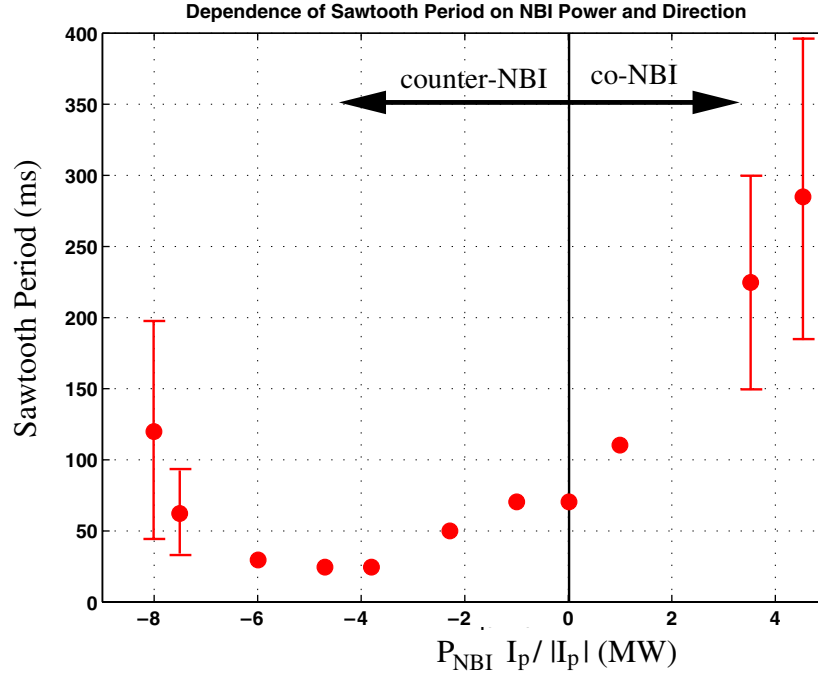
Dependence of Sawtooth Period on NBI Power and Direction

Figure 6. Showing the dependence of the sawtooth period on NBI heating power and direction relative to the plasma current in a series of dedicated JET discharges [16]. Error bars indicate variation of sawtooth period over the measured two second interval during which measurements were taken.

sawteeth, and it is found that the thermal ion kinetic contribution δW_{ki} is negligible and the hot ion kinetic term δW_{kh} is also smaller than the corresponding term for the forward B discharge 60768. Since the instability criterion equation (2) is always met, the trigger occurs when the criterion $s_1 > s_c(\beta)$ is satisfied. Since the sawtooth period is similar to that of Ohmic plasmas, it is reasonable to suppose that the energetic particles do not significantly modify the current penetration time. Furthermore, the counter current drive is small, and measurements of the inversion radius cannot discern an effect on the q profile.

Figure 6 demonstrates that it is necessary to have at least 7 MW of cntr-NBI power before kinetically stabilized sawteeth are observed. This contrasts with only requiring 2 MW of co-NBI. For discharges where the deposition of heating is concentrated deeply in the centre (e.g. with normal injection), the sawtooth period is much smaller than Ohmic sawteeth. For moderate cntr-NBI power the sawteeth are very regular, while for large cntr-NBI power or moderate co-NBI power the sawtooth period varies sigificantly (see error bars in figure 6) over the two second stationary interval during which measurements are made. A clear broad minimum in the sawtooth period is observed with a timescale less than half that of Ohmic sawteeth. The physical reason for this is as yet uncertain, but in contrast with the speculation in [11] it would appear that the relatively small and broadly deposited current drive is insignificant in all the discharges assessed here. It is possible, however, that the deep penetration of NBI ions could modify the conductivity profile in a similar way to that of on-axis ECH (see section 2.2 and figure 2). The sensitive influence of the conductivity profile on sawteeth is made possible because, unlike co-NBI where the sawtooth period is determined by the criterion for macroscopic instability [24] of equation (2), for cntr-NBI of moderate

heating power the criterion of equation (2) is always met. Hence the trigger is determined by the critical shear criterion of equation (3) together with equation (5), which, as we have seen, is particularly sensitive to changes in the local conductivity.

Finally, it is noted that there are other ways in which toroidal plasma rotation can modify stability. A similar variation of the sawtooth period with heating power and injection orientation has emerged in TEXTOR [37] and MAST [38]. However, in both TEXTOR and MAST the minimum in the sawtooth period corresponds closely to a vanishing precursor frequency, while with, e.g. 4 MW of cntr-NBI in JET the MHD mode frequency is of the same order of magnitude as the toroidal plasma rotation frequency. Furthermore, in MAST, the toroidal rotation frequency is an order of magnitude larger than JET discharges with the same NBI power, and hence it is quite possible that centrifugal effects could be important [39]. In addition, if $\Delta\Omega \sim \{\omega_{\text{mdh}}, \omega_{*\text{h}}\}$, the kinetic response of the NBI minority ions themselves could be modified significantly by sheared flow [34]. Finally, other effects which have not been considered here include the possibility that changes in the bulk plasma momentum by NBI could modify the toroidal coupling of perturbations on the 1/1 and 2/1 surfaces [40].

5. Negative ion based neutral beam injection

Experiments in JT-60U using 350 keV NNBI in the direction of the plasma current have yielded long sawteeth [17]. The dependence of the sawtooth period on electron temperature is found to be in excess of the scaling $\sim T_{\text{e}}^{3/2}$ solely due to resistive diffusion. However, these long sawteeth cannot be explained simply in terms of the usual kinetic stabilization observed for conventional NBI or RF minority ions because, for the strongly tangential injection employed, the fraction of trapped ions is presumably small. Nevertheless, the tangential injection is unbalanced, and it is found that the parallel velocity asymmetry in the distribution function gives rise to an important kinetic contribution when finite orbit effects are taken into account [18]. It is found that on-axis co-NNBI and strongly off-axis cntr-NNBI stabilize the internal kink mode, while on-axis cntr-NNBI and strongly off-axis co-NNBI are destabilizing. Here, strongly off-axis refers to the possibility of obtaining positive fast ion pressure gradients at $q = 1$. In ITER, tangential 1 MeV NNBI is being planned. It is found that [41] the stabilizing contribution from this population of NNBI ions in ITER could be as large as the stabilizing contribution from trapped alpha particles if

$$r \frac{\mathrm{d}P_{\text{h}}}{\mathrm{d}r}\bigg|_{r_1} \approx \frac{1}{\epsilon_1^{1/2}} \int_0^{r_1} \mathrm{d}r \left(\frac{r}{r_1}\right)^{3/2} \frac{\mathrm{d}P_\alpha}{\mathrm{d}r},$$

where P_{h} and P_α, respectively, refer to the pressure from unbalanced circulating NNBI hot ions and alpha particles. Such a scaling could be satisfied for tangential injection of NNBI ions where $\mathrm{d}P_{\text{h}}/\mathrm{d}r$ is peaked off-axis, i.e. close to $q = 1$. For NNBI power of 35 MW and alpha heating power of 80 MW [42] it is quite possible that one finds that $\mathrm{d}P_{\text{h}}/\mathrm{d}r > \mathrm{d}P_\alpha/\mathrm{d}r$ close to $q = 1$.

The effect of the driven current from NNBI is now briefly addressed. TRANSP simulations [42] of standard ELMy H-mode scenarios in ITER demonstrate that the NNBI population does significantly modify (broaden) the q-profile. Depending on the injection geometry employed, co-current drive with a non-monotonic profile could readily be created [43]. For such a non-monotonic NNBI current drive profile $j_{\text{NNBI}}(r)$, the safety factor in the core could increase with respect to time. This can be understood from equation (4) for which $\partial(\eta j_{\text{cd}})/\partial r > 0$ yields $\partial q/\partial t > 0$ providing that the effect of current drive dominates over conventional resistive diffusion in the core. The current drive efficiency should at the very least be sufficient to significantly delay the first creation of a $q = 1$ surface following start up. This application

of current drive could in principle, therefore, be employed in order to avoid or delay sawteeth rather than provide sawtooth control by means of destabilization.

6. Conclusions

This paper presents an overview of recent advances in the field of sawtooth control. It includes progress on sawtooth destabilization using both localized electron and ion based heating and current drive. Consistent simulations of TCV and JET discharges demonstrate that sawtooth destabilization occurs as a result of enhancement to the current diffusion close to the $q = 1$ rational surface [12]. The ability to control sawteeth, initially stabilized by an energetic trapped ion population, is a particularly important step forward given the expectation that alpha particles will lengthen sawtooth periods in ITER. Recent experiments in JET with counter-NBI highlights the influence of plasma rotation in present day tokamaks. While the expected small momentum induced flow is not predicted to strongly influence sawteeth in ITER, the effect of unbalanced NNBI is predicted to strongly stabilize sawteeth through kinetic stabilization of the internal kink mode and possibly by slowing down resistive diffusion in the core.

Acknowledgment

References

 [1] ITER Physics Basis Editors *et al* 1999 *Nucl. Fusion* **39** 2137
 [2] Campbell D J *et al* 1988 *Phys. Rev. Lett.* **60** 2148
 [3] Phillips C K *et al* 1992 *Phys. Fluids* B **4** 2155
 [4] Graves J P *et al* 2000 *Phys. Rev. Lett.* **84** 1204
 [5] Porcelli F, Boucher D and Rosenbluth M N 1996 *Plasma Phys. Control. Fusion* **38** 2163
 [6] Sauter O *et al* 2002 *Phys. Rev. Lett.* **88** 105001
 [7] Campbell D J *et al* 1988 *Proc. 15th Eur. Conf. on Controlled Fusion and Plasma Heating (EPS, Dubrovnik, 1988)* vol 12B, Part 1, p 377
 [8] Porcelli F *et al* 2004 *Nucl. Fusion* **44** 362
 [9] Bobrovskii G A *et al* 1987 *Sov. J. Plasma Phys.* **13** 665
[10] Goodman T P *et al* 1999 *Proc. 26th EPS Conf. on Controlled Fusion and Plasma Physics (Maastricht, 1999)* vol 23J (ECA) p 1101
     Henderson M A *et al* 2001 *Fusion Eng. Des.* **53** 241
[11] Edwards A W *et al* 1992 *Proc. 19th EPS Conf.* vol 16C, Part I, p 379
[12] Angioni C, Goodman T P, Henderson M A and Sauter O 2003 *Nucl. Fusion* **43** 455
[13] Mück A *et al* 2005 *Plasma Phys. Control. Fusion* **47** 1633
[14] Mayoral M-L 2004 *Phys. Plasmas* **11** 2607
[15] Eriksson L-G *et al* 2004 *Phys. Rev. Lett.* **92** 235004
[16] Nave M F F *et al* 2004 *Proc. 31st EPS Conf. on Plasma Physics (London, UK, 28 June–2 July 2004)* (European Physical Society) P1-162
[17] Kramer G J *et al* 2000 *Nucl. Fusion* **40** 1383
[18] Graves J P 2004 *Phys. Rev. Lett.* **92** 185003
[19] Reimerdes H *et al* 2000 *Plasma Phys. Control. Fusion* **42** 629
[20] Bussac M N, Pellat R, Edery D and Soulé J L 1975 *Phys. Rev. Lett.* **35** 1638
[21] Eriksson H G and Wahlberg C 2002 *Phys. Plasmas* **9** 1606
[22] Martynov An, Graves J and Sauter O 2005 *Plasma. Phys. Control. Fusion* **47** 1743
[23] Migliuolo S, Pegoraro F and Porcelli F 1991 *Phys. Fluids* B **3** 1338
     Zakharov L, Rogers B and Migliuolo S 1993 *Phys. Fluids* B **5** 2498
[24] Angioni C *et al* 2002 *Plasma Phys. Control. Fusion* **44** 205

[25] Levinton F M, Zackharov L, Batha S H, Manickam J and Zarnstorff M C 1994 *Phys. Rev. Lett.* **72** 2895
[26] Kadomsev B B 1977 *Sov. J. Plasma Phys.* **1** 555
[27] Gimblett C G and Hastie R J 1994 *Plasma Phys. Control. Fusion* **36** 1439
[28] Buttery R J *et al* 2004 *Nucl. Fusion* **44** 1027
[29] Weller A *et al* 1987 *Phys. Rev. Lett.* **59** 2303
[30] Bhatnagar V P *et al* 1994 *Nucl. Fusion* **34** 1579
[31] Porcelli F *et al* 1993 *Proc. EPS Conf.* vol 16C, Part II, p 901
[32] Eriksson L-G *et al* 1998 *Phys. Rev. Lett.* **81** 1231
[33] Mantsinen M *et al* 2002 *Phys. Rev. Lett.* **88** 105002
[34] Graves J P *et al* 2003 *Phys. Plasmas* **10** 1034
[35] Graves J P, Hastie R J and Hopcraft K I 2000 *Plasma Phys. Control. Fusion* **42** 1049
[36] Bailey D 1998 *Report* JET-R 04
[37] Koslowski H R 2005 *Fusion Sci. Technol.* **47** 260
[38] Akers R J *et al* 2005 *32nd EPS Conf. on Plasma Physics (Tarragona, 27June–1 July 2005)* ECA vol 29C P-2.062
[39] Wahlberg C and Bondeson A 2000 *Phys. Plasmas* **7** 923
     Kleva R G and Guzdar P N 2002 *Phys. Plasmas* **9** 3013
[40] Fitzpatrick R, Gimblett C G and Hastie R J 1993 *20th EPS Conf. on Plasma Physics and Contolled Fusion (Lisbon)* vol 17C, Part IV, p 1335
[41] Graves J P 2005 *Phys. Plasmas* **12** 090908
[42] Budny R V 2002 *Nucl. Fusion* **42** 1383
[43] Tobita K *et al* 2004 *Plasma Phys. Control. Fusion* **46** S95